



**HAL**  
open science

## Alkali-silica reaction (ASR) expansion: Pessimism effect versus scale effect

Xiao Xiao Gao, Stéphane Multon, Martin Cyr, Alain Sellier

### ► To cite this version:

Xiao Xiao Gao, Stéphane Multon, Martin Cyr, Alain Sellier. Alkali-silica reaction (ASR) expansion: Pessimism effect versus scale effect. *Cement and Concrete Research*, 2013, 44, pp.25–33. 10.1016/j.cemconres.2012.10.015 . hal-01724652

**HAL Id: hal-01724652**

**<https://hal.insa-toulouse.fr/hal-01724652>**

Submitted on 23 Mar 2018

**HAL** is a multi-disciplinary open access archive for the deposit and dissemination of scientific research documents, whether they are published or not. The documents may come from teaching and research institutions in France or abroad, or from public or private research centers.

L'archive ouverte pluridisciplinaire **HAL**, est destinée au dépôt et à la diffusion de documents scientifiques de niveau recherche, publiés ou non, émanant des établissements d'enseignement et de recherche français ou étrangers, des laboratoires publics ou privés.

# Alkali-silica reaction (ASR) expansion: pessimum effect versus scale effect

Xiao Xiao Gao <sup>a</sup>, Stéphane Multon <sup>a\*</sup>, Martin Cyr <sup>a</sup>, Alain Sellier <sup>a</sup>

<sup>(a)</sup> *Université de Toulouse; UPS, INSA; LMDC (Laboratoire Matériaux et Durabilité des Constructions); 135, avenue de Rangueil; F-31 077 Toulouse Cedex 04, France*

---

## Abstract

The effect of aggregate size on ASR expansions has been largely studied and conflicting results exist concerning the aggregate size that leads to the highest ASR expansion. Most of the research works clearly show a pessimum effect of aggregate size on ASR expansion. However, all the results available in the literature were obtained using different experimental conditions and the combined effects of other important parameters, such as specimen size used in the expansion tests, have often been neglected. This paper aims to investigate the combined effect of specimen size and aggregate size on ASR expansion. Experimental results highlight a scale effect, a combination of the effects of aggregate size and specimen size on ASR expansion. This scale effect appears to be influenced by the reactive silica content of the aggregate. Modelling at microscopic level is used to propose a quantification of this effect.

**Keywords:** alkali-silica reaction (ASR), particle size, specimen size, expansion, scale effect

---

\* Corresponding author. *e-mail address:* multon@insa-toulouse.fr (Stéphane Multon)

## 27 **1. Introduction**

28 Alkali-Silica Reaction (ASR) is a deleterious chemical reaction occurring in all types of  
29 structures that contain alkali-reactive aggregates: dams, bridges, roads, breakwaters, etc. The  
30 mechanism of expansion can be described in three main steps [1-4]: the diffusion of ionic  
31 species ( $\text{Na}^+$ ,  $\text{K}^+$ ,  $\text{OH}^-$ ,  $\text{Ca}^{2+}$ ) into the aggregates, the disruption of the silanol and siloxane  
32 bonds contained in the reactive silicate, and the reaction of alkali silicate with ionic species  
33 ( $\text{Na}^+$ ,  $\text{K}^+$ ,  $\text{Ca}^{2+}$ ) to form ASR gels. ASR gel induces pressure in the aggregate and in the  
34 cement paste, leading to stresses and thus cracking. ASR expansion depends on numerous  
35 parameters (amounts of alkali, reactive silica and water present, aggregate and specimen sizes,  
36 etc.).

37 It seems that the range of aggregate size causing the highest ASR expansion varies with the  
38 nature and composition of the aggregate. Numerous papers [5-23] discuss the effect on ASR  
39 expansion of particle sizes of reactive aggregates like opal [5-12], various kinds of silica  
40 glass, fused silica and waste silica glass, and so on [13-24]. Some research has shown that the  
41 expansion induced by ASR increases as the reactive particle size is reduced [9,14,17,19].  
42 Some authors obtained insignificant expansion when the sizes of the reactive particles were  
43 under 50 to 150  $\mu\text{m}$  [11,13,15,22]. Furthermore, the use of powder from reactive aggregates  
44 like pozzolans, with particle sizes up to about 100  $\mu\text{m}$ , has been developed to counteract the  
45 effect of ASR [15,18,21]. Only a few exceptions with very small particles led to significant  
46 ASR expansions, all involving opal aggregates [5-7, 12]. Other research works have shown a  
47 pessimum effect for various types of aggregates, with pessimum values occurring in a wide  
48 interval of particle sizes [4,7,8,10-13,16,20,23,24]. It is observed that, in some cases, the most  
49 damaging size, leading to the highest ASR expansion, reaches more than 1 mm. The effect of  
50 “specimen size” has been much less studied [25-28]. Experiments performed with different

51 'aggregate size to specimen size' ratios show the effect of the size of the specimens on the  
52 ASR expansions measured. Lower expansions were measured on the smaller specimens  
53 [25,26].

54 First, a literature review showed that conflicting results exist concerning the most damaging  
55 reactive aggregate size, which leads to the highest ASR expansion. Secondly, experimentation  
56 performed by Zhang et al. [26] suggested that the two effects of aggregate and specimen sizes  
57 are combined. Therefore, the difficulty in generalizing results on the effect of the particle size  
58 of reactive aggregates could be explained by the differences in experimental conditions, and  
59 particularly the combined effects of aggregate size and specimen size on ASR expansion. This  
60 paper aims to investigate and quantify this scale effect and the influence the reactive silica  
61 content of aggregate has on the effect, in order to gain a better understanding of expansion  
62 tests.

63 The development of an ASR model at the microscopic level is a major concern of researchers  
64 trying to understand the mechanisms involved in the ASR and to predict future expansion.  
65 Previous modelling investigated the different aspects of the reaction: the mechanical  
66 consequences of ASR [29-32], the chemical mechanisms driving the attack of the aggregate  
67 by hydroxyl ions [33] and their coupling [34-38]. These works do not take into account the  
68 permeation of ASR gels in cracks which could be the main cause of the decrease of expansion  
69 by pessimum or scale effects. The concepts of fracture mechanics can explain the cracking  
70 phenomenon in the cases of aggregate in infinite matrix [39, 40] or of central penny-shaped  
71 crack in sphere [41]. However, it is difficult to apply such models in the cases of specimens  
72 containing aggregates with numerous interactions (interactions with other neighbour  
73 aggregates and with specimen boundaries). The experiments presented in this paper were used  
74 to point out the dependence of expansion with aggregate and specimen sizes. These results are  
75 explained by fracture mechanics concepts. The teachings pointed out by fracture mechanics

76 are then used to propose a simplified relationship to take into account the scale effect in an  
77 analytical modelling. Finally, the experimental results are used here to calibrate and discuss  
78 the validity and the capability of the model.

## 79 **2. Experimental conditions and results**

### 80 ***2.1 Experimental conditions***

81 Expansion was measured on mortar prisms with a water/cement ratio of 0.5 and a sand (1512  
82 kg/m<sup>3</sup>) / cement (504 kg/m<sup>3</sup>) ratio of 3. Mixtures were adjusted by adding NaOH to the  
83 mixing water in order to have the same alkali concentration in the pore solution and in the  
84 storage solution. For the reference specimens, the sand was composed of the non-reactive  
85 marble only. For all the other specimens, the sand contained 30% of reactive aggregate and 70%  
86 of non-reactive marble. The prisms were stored in NaOH solution at 60°C. The expansion  
87 measurements were performed after the prisms had cooled to 20°C (~12 h) in the NaOH  
88 solution. Each variation of length value was calculated as the mean of three values from three  
89 replicate specimens measured using the scale micrometer method (specimens had shrinkage  
90 bolts in the two extremities) [42,43]. The experimentation presented in this paper aimed to  
91 study three particular points:

#### 92 ***Effect of alkali concentration***

93 As explained above, the specimens were kept immersed in NaOH solution. The aim of this  
94 part was to study three NaOH concentrations for immersion close to the standard conditions  
95 of 1 mol/l (0.77, 1 and 1.25 mol/l). Reactive siliceous limestone was used to study the effect  
96 of alkali concentration on ASR expansion. The specimen and aggregate sizes were  
97 respectively 20 x 20 x 160 mm and 315-1250 µm (15% of 315-630 and 15% of 630-  
98 1250 µm). Eighteen specimens (nine reactive and nine reference specimens) were used for  
99 this part of the experimentation.

## 100 *Effect of reactive silica content*

101 The second point concerned the effect of the reactive aggregate nature on ASR expansion.  
102 Four reactive aggregates with different reactive silica contents were chosen and tested. Opal  
103 (O) is known to be very reactive and to give large expansion if the amount of available alkali  
104 is sufficient. Quartzite (Q) and siliceous limestone (SL) are usually less reactive but can  
105 exhibit significant expansion in concrete. Quartz aggregate (QA), which contains mostly  
106 quartz, is considered as non-reactive. The silica contents of the aggregate [43] are given in  
107 Table 1. The aggregates were used to cast 20x20x160 mm specimens with 315-1250  $\mu\text{m}$   
108 reactive aggregate (15% of 315-630 and 15% of 630-1250  $\mu\text{m}$ ). The fifteen specimens were  
109 kept in 1 mol/l NaOH solution.

## 110 *Combined effect of aggregate and specimen sizes*

111 Four reactive aggregate size classes: C1 (0-315  $\mu\text{m}$ ), C2 (315-630  $\mu\text{m}$ ), C3 (630-1250  $\mu\text{m}$ )  
112 and C4 (1250-2500  $\mu\text{m}$ ) and three specimen sizes: 20x20x160 mm, 40x40x160 mm and  
113 70x70x280 mm were used to research the combined effect of aggregate and specimen sizes on  
114 ASR expansion. The forty-five specimens (thirty-six reactive and nine non-reactive  
115 specimens) were stored in 1 mol/l NaOH solution. Siliceous limestone was used as the  
116 reactive aggregate.

## 117 **2.2 Experimental results**

### 118 **2.2.1 Effect of the alkali concentration**

119 The final expansions for the three NaOH concentrations of 0.77, 1.0 and 1.25 mol/l were  
120 0.67%, 0.64% and 0.60% respectively (Figure 1). The difference between two consecutive  
121 concentrations appeared to be small considering that the standard deviation for the specimens  
122 was in the range of 0~0.02%. Between 0.77 and 1.25 mol/l, the alkali concentrations could be  
123 considered to have little influence on ASR expansions in conditions of abundant alkali.

124

### 125 **2.2.2 Effect of the reactive silica content**

126 The ASR expansions obtained for the four aggregates are plotted in Figure 1. The specimens  
127 containing opal were the most reactive, with fast expansion and an asymptotic value of about  
128 1.35%. The specimens with siliceous limestone exhibited rapid expansion, but the final  
129 expansions were lower (about 0.6%). The specimens with quartzite aggregate presented a  
130 slow expansion rate but reached a final expansion of about 0.55%. ASR expansion of the  
131 specimens containing quartz aggregate was about 0.14%. By the end of the experiment, the  
132 specimens containing opal were seriously damaged and cracked (crack width of about 425  $\mu\text{m}$ )  
133 while the other specimens showed cracks with widths smaller than 10  $\mu\text{m}$  (Figure 2). The  
134 reliability of measured expansions could have been affected by such cracking. However, the  
135 coefficient of variations obtained for three specimens was lower than 5%. It shows that the  
136 expansion scattering stayed quite small in spite of the large cracks.

### 137 **2.2.3 Combined effects of aggregate and specimen sizes**

138 The ASR expansions obtained for mortars containing the reactive siliceous limestone with  
139 various aggregate sizes and cast in specimens of different sizes are given in Figure 3. First,  
140 the specimens containing small reactive particles (0-315  $\mu\text{m}$ ) had the smallest expansion  
141 (lower than 0.15%), confirming results found in the literature. The ASR expansions were  
142 significant and higher than 0.5% for the other three aggregate sizes. Concerning final ASR  
143 expansion, the largest specimens showed the highest ASR expansion (Figure 4). This was  
144 particularly significant on the large aggregate class 1250-2500  $\mu\text{m}$  (ASR expansions were  
145 twice as large for the 70x70x280-mm specimens as for the others). Moreover, ASR  
146 expansions presented a pessimum effect with the reactive aggregate size (with a final  
147 expansion larger for the aggregate size 315-630  $\mu\text{m}$  than for 1200-2500  $\mu\text{m}$ ) for  
148 measurements performed on the smallest specimens (20x20x160 mm, 40x40x160 mm) but

149 not for the largest ones (Figure 4). These observations show the significant combined effect of  
150 specimen size and aggregate size.

#### 151 **2.2.4 Scale effect**

##### 152 *Mechanisms*

153 In order to understand the scale effect (combination of the aggregate- and specimen-size  
154 effects on expansion), the ASR development can be described in four phases:

155 1. Ions (hydroxyls and alkalis) from the pore solution diffuse into the aggregates whatever the  
156 reactive silica distribution in the aggregate (uniform or in veins – Figure 5-a).

157 2. Ions react with reactive silica and ASR gel is created in and/or around the aggregate  
158 (according to the distribution of the reactive silica in the aggregate, a part of the reactive silica  
159 can even be in direct contact with cement paste – Figure 5-b). A part of the gel can fill the  
160 connected porous volume surrounding the aggregate without leading to damage [33-35,39]  
161 (Figure 5-b) and also a part of the porosity of the aggregate close to the reactive site which  
162 can lead to the cracking of veined aggregates [41]. This can explain why the smallest  
163 aggregates lead to small expansion. For the same reactive silica content, more of the gel can  
164 migrate in the connected porosity for the smallest aggregates than for larger aggregates. Thus,  
165 a small amount of ASR gel is able to cause expansion [23,34,39]. It is easier for the cement  
166 paste to accommodate ASR gel when the gel is created by a large number of small sites rather  
167 than by a small number of scattered, larger sites.

168 3. ASR gel exerts pressures on the surrounding aggregate and cement paste when a part of the  
169 connected porosity is filled (Figure 5-c) and the gel can no longer move in the porosity. In  
170 order to assess the gel pressure  $p_g^a$  for the aggregate of size  $a$ , an analogy with previous  
171 modelling [23, 34] can be made. In these works, the ASR mechanical effect was assumed to  
172 be an imposed strain of the aggregate on the surrounding cement paste equal to:



$$\mathcal{E}_{imp}^a = \frac{\langle V_a^{gel} - V_a^{poro} \rangle^+}{V_a} \quad (1)$$

173  $\langle X \rangle^+$  is the positive part of  $X$ : if  $X < 0$ ,  $\langle X \rangle^+ = 0$  otherwise  $\langle X \rangle^+ = X$

174  $V_a^{gel}$  is the volume of ASR gel formed in reactive aggregates and  $V_a$ , the volume of the  
 175 reactive aggregate,  $V_a = \frac{4}{3}\pi \cdot R_a^3$  (if spherical shape is assumed for aggregate).

176  $V_a^{poro}$  is the volume of the porosity in which the ASR gel can migrate without causing  
 177 expansion. It was assumed that the proportion of gels filling the porosity connected to the  
 178 reactive sites (cement paste and aggregate) without creating pressure was the total volume of  
 179 porosity filled by the gel with an equivalent thickness  $t_c$ , which was assumed to be  
 180 independent of the aggregate size:

$$V_a^{poro} = \varphi \frac{4}{3}\pi \cdot \left( (R_a + t_c)^3 - R_a^3 \right) \quad (2)$$

181 where  $\varphi$  is the porosity of the mortar. In reality, it includes a part of aggregate porosity but, by  
 182 sake of simplicity, the model considers the thickness  $t_c$  as the average distance of gel  
 183 penetration which should depend on the gel pressure: penetration is more or less difficult due  
 184 to the ASR gel viscosity, its surface tension and the size of the pores of the aggregate and of  
 185 the cement paste surrounding the reactive sites [39]. Once the gel reaches  $t_c$ , it cannot  
 186 penetrate in the paste anymore due to the combination of these three main parameters. They  
 187 were assumed to be the same for all the aggregates and that's why the equivalent thickness  $t_c$   
 188 was assumed to be independent with the aggregate size.

189 In order to assess the effect of ASR-gel on the cement paste in term of pressure, similar  
 190 relationship can be used.  $p_g^a$ , the gel pressure can be assumed to be proportional to  $M_g$  the gel  
 191 bulk modulus and to the increase of volume due to ASR-gel production:

$$p_g^a(t) = M_g \left\langle V_a^{gel} - \varphi \frac{4}{3}\pi \left[ (R_a + t_c)^3 - R_a^3 \right] \right\rangle \quad (3)$$

192  $V_a^{gel}$ , the volume of ASR gel formed in reactive aggregates, is proportional to the number of  
 193 moles of ASR gel formed after the attack of the reactive silica:

$$V_a^{gel} = n_a^{gel} \cdot V_{gel}^{mol} \quad (4)$$

194 with  $n_a^{gel}$  (mol): the number of moles of ASR gel produced by the aggregate  $a$  and  $V_{gel}^{mol}$   
 195 ( $m^3/mol$ ): the molar volume of the gel.

196 The number of moles of ASR gels produced by the reaction is defined by the number of  
 197 moles of silica attacked by alkalis and can be taken proportional to  $s$  the reactive silica content  
 198 (in mol/ $m^3$ ):

$$n_a^{gel} = \frac{4}{3} \pi R_a^3 \cdot s \cdot \zeta(t) \quad (5)$$

199  $\zeta(t)$  is the chemical advancement of the alkali-silica reaction (which depends on temperature,  
 200 moisture and alkali conditions and is assessed by the diffusion of ionic species in the  
 201 aggregate and by the time necessary for the attack of the reactive silica by hydroxyl ions and  
 202 for the formation of ASR-gels [34]).

203 Finally,  $p_g$ , the gel pressure at the time-step  $t$ , can be assessed from:

$$p_g^a(t) = M_g \left\langle \frac{4}{3} \pi R_a^3 \cdot V_{gel}^{mol} \cdot s \cdot \zeta(t) - \varphi \frac{4}{3} \pi [(R_a + t_c)^3 - R_a^3] \right\rangle \quad (6)$$

204 4. The pressure causes cracking of the aggregate and cement paste. Whatever the reactive  
 205 silica distribution in the aggregate, the propagation of cracks in small specimens containing  
 206 large aggregate can be rapid and can occur for low pressures, while the propagation is more  
 207 difficult for larger specimens containing smaller aggregates and needs higher pressure (Figure  
 208 5-d). In the framework of fracture mechanics [44-45], the maximal normal stress in the  
 209 vicinity of an inclusion (e.g. the aggregate) that induces pressure on a matrix (e.g. the cement  
 210 paste) is given by:

$$\sigma(r) = \frac{K_I}{\sqrt{2\pi r}} \quad (7)$$

211 With  $\sigma$ , the maximal normal stress at the point M located at distance  $r$  from the edge of the  
212 inclusion (Figure 5-d) and  $K_I$ , the stress intensity factor obtained for a specimen in stress-free  
213 conditions from the relation:

$$K_I = p_g^a \cdot f\left(\frac{R_a}{L}\right) \quad (8)$$

214 where  $f$  is a function increasing with the ratio  $R_a/L$  (which can be obtained in [41]), with  $R_a$   
215 the aggregate radius and  $L$  the dimension of the specimen ( $a$ : superscript relative to the size of  
216 the reactive aggregate).

### 217 ***Smaller expansion in smaller specimen***

218 The larger the aggregate size compared to the specimen size, the larger the normal stress at a  
219 given distance from the aggregate (Equations 7 and 8). Thus, the tensile strength at the  
220 boundary of the specimen can be reached for a smaller pressure (Figure 5-d) and cracks can  
221 be initiated earlier. Once concrete cracks, ASR-gels can be accommodated by cracking  
222 without creating supplementary pressure [46,47] and can even leach off through the porosity  
223 induced by cracking. Thus, the pressure in the gels falls, which stops the expansion.

224 If the pressure necessary to cause cracks is lower for small specimens containing large-sized  
225 aggregate, the pressure of the gel will fall sooner in the case of the 20x20x160-mm specimens  
226 containing the 1250-2500- $\mu\text{m}$  aggregate than for the 70x70x280-mm specimens containing  
227 the same aggregate, and thus cause smaller expansion.

### 228 ***Pessimum effect or scale effect***

229 The scale effect can also explain the pessimum effect of ASR expansion with aggregate size.  
230 For the largest aggregates, a part of the difference of expansion can be explained by a delay in  
231 the attack of the reactive silica by the hydroxyl ions due to the diffusion of the ions into the  
232 aggregate [23]. Measurements confirmed that the expansion rate was slower in the largest  
233 particles whatever the size of the specimens (Figure 3). However, even when the final value  
234 was reached, ASR expansion remained lower for the largest aggregates in the smallest

235 specimens. As explained above, the 20x20x160-mm specimens containing the 1250-2500- $\mu$ m  
236 aggregate were more affected by the scale effect than the specimens containing the 315-630-  
237  $\mu$ m aggregate: a larger aggregate induced a greater stress intensity factor (Equation 8).  
238 Therefore, the part of reactive silica consumed when cracking appeared is lower when  
239 cracking appears in the specimens containing the largest aggregate. Once cracking occurs, the  
240 gel is accommodated by the cracks and the gel produced after cracking leads to little  
241 supplementary pressure. Expansion ceases before the chemical reaction stops, giving a final  
242 expansion lower than that for the largest aggregate. This is consistent with the experimental  
243 determination of the degree of reaction performed with chemical attack [47] and SEM image  
244 analysis [48]: expansion stopped while the degree of reaction was still increasing. The  
245 pessimum effect versus specimen size is not an intrinsic phenomenon; it is due to the scale  
246 effect, which depends on the 'specimen size to aggregate size' ratio. In this experimentation,  
247 only mortars were tested and the pessimum effect disappeared for aggregate of 1.25-2.5 mm  
248 when tests were performed in specimens of 70 mm. For concrete, the pessimum still exists for  
249 aggregate of 4-8 mm in specimens of 70 mm [24]. If the scale effect (combination of the  
250 aggregate size effect and the specimen size effect) is identical for concrete, specimens of more  
251 than 250 mm could be necessary to remove the pessimum effect for such aggregates.  
252 Supplementary investigations are necessary to analyse this effect on concrete.

### 253 *Effect of the reactive silica content on the scale effect*

254 At last, it can also be used to analyse the effect of the reactive silica content on ASR  
255 expansion (Figure 1). As shown in Figure 6, the final expansions measured on specimens  
256 containing the different aggregates were not proportional to the reactive silica content.  
257 Moreover, the specimens containing opal were much more damaged and cracked than those  
258 with the other aggregates. This could have been due to the large concentration of reactive  
259 silica contained in opal. A larger reactive silica content would induce a higher gel pressure

260 (Equation 6) and thus a greater stress intensity factor (Equation 8) for opal than for the  
261 siliceous limestone. Therefore, the ratio between the total reactive silica and the reactive silica  
262 consumed when cracking appeared was not the same. The part of reactive silica consumed  
263 would be lower when cracking appeared in the specimens containing opal than in the  
264 specimens containing the siliceous limestone. Once cracking had occurred, cracks  
265 accommodated the gel, and expansion stopped before the chemical reaction finished, without  
266 proportionality with the total reactive silica. This effect was probably very important in the  
267 case of specimens containing opal in which cracks were very large at the end of the  
268 experiment (Figure 2).

269 The concept of stress intensity factor appears to be important for an understanding of the  
270 development of ASR expansion in concrete. The larger the stress intensity factor  $K_I$  is, the  
271 faster cracks appear and the cracking could lead to reduction of the expansion through gel  
272 accommodation and exudation. The ratios between specimen and aggregate sizes were very  
273 high in these experiments. This shows that it could be difficult to use specimens large enough  
274 to avoid the scale effect. One possibility would be to try to control the aggregate and the  
275 specimen sizes so as to perform the test with similar stress intensity factors and thus to have  
276 similar cracking conditions as proposed in [42,43] but this would be difficult to do,  
277 particularly as far as controlling the aggregate size is concerned. Another possibility is to  
278 understand the scale effect through a model that can be used to analyse expansion tests. This  
279 is the aim of the modelling presented in the next part.

### 280 **3. Modelling ASR expansion**

281 The model used in this paper is an improvement on the microscopic model [34]. It was based  
282 on previous models [33, 35-37,39] and attempted to predict the damage and the expansion of  
283 a Representative Elementary Volume (REV) of concrete containing a mix of reactive

284 aggregates of different sizes. The reaction between the reactive silica and the alkali was  
285 determined through the mass balance equation, which describes the diffusion mechanism in  
286 the aggregate and the fixation of the alkali in the ASR gels. The mechanical part of the model  
287 is based on damage theory in order to assess the decrease of stiffness of the mortar due to  
288 cracking caused by ASR and to calculate the expansion of the REV [34]. Some modifications  
289 were made in this model: the threshold of alkalis was re-evaluated in accordance with the  
290 results present above and the combined effects of specimen and aggregate sizes and reactive  
291 silica content on expansions were taken into account.

## 292 ***3.1 Presentation of the model***

### 293 ***3.1.1 Diffusion of alkali***

294 The diffusion of ions in the aggregate partly controls the kinetics of the chemical attacks and  
295 of the expansion. At the beginning of ASR, hydroxyl ions attack the reactive silica of the  
296 aggregate. Hydroxyl ions come from the pore solution and thus the external boundary of the  
297 reactive aggregates is attacked first. If the reactive silica is uniformly distributed in the  
298 aggregate, the reactive silica closest to the pore solution is attacked first (Figure 5-a top). If  
299 the reactive silica occurs in veins, the penetration of hydroxyl ions is not uniform but veins in  
300 contact with the pore solution are attacked first (Figure 5-a bottom). Therefore, in both cases,  
301 the transport of ionic species in the aggregate can be modelled by an equivalent diffusion of  
302 ions from the pore solution to the aggregate core. The diffusion is not the only phenomenon  
303 which impacts the kinetics of ASR-expansion: the time necessary for the attack of the reactive  
304 silica by hydroxyl ions and for the formation of ASR-gels is taken into account through a  
305 depletion term in the mass balance equation [34]. This term models the alkali consumed by  
306 the ASR-gel formation. This alkali consumption is assumed to be linear with the alkali  
307 concentration in the aggregate. The temperature of storage for the experiment was 60°C. It  
308 accelerates ASR considerably compared to the environmental conditions of real damaged

309 structures and can affect the nature of the gel. It impacts the values of the kinetic parameters  
310 but should not affect the principle of the modelling.

311 As in the previous model [34], only the diffusion of ions in the aggregate was considered  
312 since the kinetics of diffusion in aggregates was much slower than in cement paste [35].  
313 Therefore, the alkali concentration at the surface of aggregates was assumed to be equal to the  
314 concentration of the NaOH solution. The kinetics of the expansion was thus partly controlled  
315 by the diffusion in the aggregate, which is one of the kinetic parameters of the model. This  
316 assumption is relevant for small specimens or when there is no chemical exchange with the  
317 environment but it can be discussed for larger specimens immersed in NaOH solution. In the  
318 experiments presented here, the largest specimens showed the slowest rate of ASR-expansion  
319 (Figure 3). This can be explained by the diffusion of the alkali into the specimens. The initial  
320 alkali concentration in the pore solution was sufficient to initiate the reaction. Alkalis were  
321 quickly consumed by the ASR gel and supplementary alkalis were necessary to maintain gel  
322 production. The alkali came from the solution and diffused into the mortar. Thus, more time  
323 was necessary for alkali to reach the centres of the largest specimens than the centres of  
324 smaller ones. Thus an alkali gradient appeared in the specimens. In consequence, at a given  
325 time, a gradient of expansion existed between aggregates located close to the external  
326 boundary and aggregates located in the core of the specimen. Only complete discretization of  
327 the whole specimen [24,31,32] would allow this difference of expansion to be considered.  
328 The aim of the modelling used in this paper was to evaluate the material behaviour that could  
329 be represented by measurements performed on small specimens. Therefore, the phenomenon  
330 of diffusion in the specimen was not taken into account. This modelling can give a good  
331 representation of the expansion kinetics of concrete damaged by ASR measured on small  
332 specimens (with width smaller than 40 mm, for which the effect of the alkali gradient is  
333 negligible).

### 334 **3.1.2 Threshold of alkali concentration**

335 In the previous model, a threshold of alkali concentration of 0.625 mol/l of Na<sup>+</sup> was  
336 considered, under which ASR did not occur [34]. It was based on experimental data showing  
337 that, with an alkali content lower than 3 kg per m<sup>3</sup> of concrete, no ASR-expansion was  
338 observed [49-52]. In tests performed in non-saturated conditions (in air with RH above 95%),  
339 the concentration of alkali played an important role in the attack of the silica. In the present  
340 work, all the specimens were kept immersed in alkali solution and, thus, the alkali was  
341 supplied in abundant quantities. The experiments performed on specimens immersed in three  
342 alkali concentrations (0.77, 1 and 1.25 mol/l) showed negligible differences. Considering a  
343 threshold of 0.625 mol/l, the expansion of the mortars kept in 0.77 mol/l solution should be  
344 significantly slower than the expansion of the mortars kept in 1.25 mol/l solution. With this  
345 threshold, the alkali concentration in the aggregate has to be higher than 0.625 mol/l before  
346 the reactive silica is attacked. The gel production kinetics is then proportional to the  
347 difference between the alkali concentration in the paste and the threshold. The alkali  
348 concentration gradient between the paste and the aggregate remains too small to induce the  
349 same reaction speed as for the other concentrations. This is not in accordance with the  
350 expansion kinetics measured on specimens (Figure 1). Therefore, the gradient must be close  
351 for the three concentrations and consequently the alkali consumption by the silica must begin  
352 as soon as alkalis are present in the aggregate, without a threshold. The result of this  
353 assumption is shown in Figure 7: if no threshold is taken into account, the expansions  
354 determined by the modelling at 50 days are of the same order as the expansions obtained for  
355 the measurements. The apparent threshold effect observed in experimentations [49-52] can be  
356 explained by the alkali fixation in C-S-H. This fixation consumed a part of alkali which are no  
357 more available in the pore solution and reduced the attack kinetics and consequently the ASR-



358 expansion kinetics. All these phenomena can be explained without considering a threshold of  
359 alkali concentration for the attack of the silica.

### 360 **3.1.3 Effective ASR-gel**

361 The ASR expansion calculated by the model is imposed by the effective volume of ASR-gel.  
362 The effective volume of gel is deduced from the total volume of gel, which is proportional to  
363 the number of moles of ASR gel formed after the attack of the reactive silica (Equation 7).  
364 Once cracking appears in the specimens, a part of the rest of the gel  $\langle V_a^{gel} - V_a^{poro} \rangle$  is  
365 assumed to be accommodated by cracks created in the aggregate and in the cement paste by  
366 the ASR-gel pressure. This gel accommodation by cracks stops the increase of the ASR-gel  
367 pressure. This part depends on the scale effect: the larger the aggregate in comparison to the  
368 specimen, the greater the volume of ASR gel accommodated. This phenomenon is also  
369 affected by the reactive silica content of the aggregate. As explained in the analysis of the  
370 experiments, the greater the reactive silica content is, the stronger is the non-linearity due to  
371 cracking. Fracture mechanics concepts show that the aggregates closest to the external  
372 boundary are the first to produce cracks. In order to quantify this effect, it can be assumed that  
373 these aggregates lead to less pressure than the aggregates located in the core of the specimens.  
374 As for the diffusion in cement paste, this will lead to a gradient of deformation between the  
375 external boundary and the core and thus to internal stresses. The scale effect appears to be a  
376 highly non-linear phenomenon. Therefore, an exponential function is proposed to model the  
377 consequences on ASR expansions. An empirical relationship to quantify the reduction of the  
378 gel amount effectively used to assess the pressure is thus assumed and applies equally to all  
379 the aggregates of a given size  $i$  without consideration for their location compared to the  
380 specimen boundary:

$$V_a^{eff} = \langle V_a^{gel} - V_a^{poro} \rangle^+ \times \max \left[ \exp \left( -c \frac{2R_a}{L} s^x \right) \right] \quad (9)$$

381 With  $V_a^{eff}$ : the effective volume of gel,  $c$ : the scale effect fitting coefficient and  $\chi$ : the silica  
382 content exponent.

383 The pressure imposed on the aggregate and thus on the cement paste depends on the effective  
384 volume of gel. Moreover, if the distribution of the reactive silica is uniform in the aggregate,  
385 the pressure will be isotropic (Figure 5-c). If the reactive silica is contained in veins in the  
386 aggregate, the large number of aggregate particles in the specimens means that the orientation  
387 of the veins in the specimens is randomly distributed and the mean resulting pressure can be  
388 considered as isotropic too (Figure 5-c). The effective volume of gel is then used in the  
389 mechanical model presented in [34] to deduce the resulting expansion.

## 390 **3.2 Comparison with experiments**

### 391 **3.2.1 Parameters**

392 Table 2 sums up the parameters used in the modelling, stating the symbols, the methods used  
393 for the identification, the values and the units. Three parameters (unique, independent of the  
394 other variables, and usable for all experiments and all aggregate types studied in this work) of  
395 the physicochemical modelling (thickness of the connected porous interface zone  $t_c$ , molar  
396 volume of ASR gel  $V_{gel}^{mol}$ , and scale effect fitting coefficient  $c$  – equations 4, 6 and 9) were  
397 obtained by curve fitting on the final expansions measured on the specimen of size 70 x 70 x  
398 280 mm with the four different size classes (0-315, 315-630, 630-1250 and 1250-2500  $\mu\text{m}$ ) of  
399 siliceous limestone (SL – Figure 8). The parameters were first determined without  
400 considering the effect of the silica content exponent ( $\chi = 0$ ) since the specimens involving the  
401 curve fitting contained the same aggregate. Once these three parameters had been assessed,  
402 the value of  $\chi$  was determined by fitting the final expansion of mortars containing opal as  
403 aggregate (O – Figure 8). As explained above, the coefficient of alkali diffusion in aggregate,  
404  $D_a$ , was used as a kinetic parameter. This coefficient can depend on the nature of the  
405 aggregate. It was obtained by curve fitting the results obtained on specimens of size 20 x 20 x

406 160 mm (Figure 9). The coefficients of diffusion in aggregate ( $D_a$ ) thus obtained by curve  
407 fitting were respectively equal to  $2.0 \times 10^{-15}$ ,  $5.0 \times 10^{-14}$ ,  $4.0 \times 10^{-16}$  and  $2.0 \times 10^{-16}$  m<sup>2</sup>/s for  
408 the siliceous limestone, opal, quartzite and quartz aggregate. It can be noted that the values  
409 were considerably lower than the usual value of diffusion coefficient determined for cement  
410 paste (about  $10^{-12}$  m<sup>2</sup>/s); the assumption of fast alkali supply at the surface of aggregate is thus  
411 verified. However, these values appear to be very small compared to coefficient of diffusion  
412 measured for quartzite [53]. It can be explained by the assumption used to determine the  
413 kinetics of the formation of ASR-gels. In this modelling, the kinetics was driven by two main  
414 phenomena: the diffusion of ions in the aggregates and the kinetics of the attack of reactive  
415 silica by alkali and hydroxyl [34]. The attack was assumed to be linear with the alkali  
416 concentration in the aggregate and only one parameter was used for all the aggregates. This  
417 parameter was fitted for siliceous limestone [34]. In the reality, the mechanisms leading to the  
418 gel formation are more complex and this simplified assumption can be responsible of the  
419 overestimation of the speed of the silica attack. It can lead to underestimation of the speed of  
420 diffusion. Improvements of the assumed kinetics of silica attack could lead to more realistic  
421 coefficients of diffusion for aggregates. However, this kinetics of silica attack could depend  
422 on the nature of the reactive silica and on the pH of the pore solution and several parameters  
423 could be necessary to obtain relevant results which could be very difficult to measure.

### 424 **3.2.2 Calculations**

425 Expansions obtained by modelling are compared with the measurements in Figures 9 and 10.  
426 Figure 9 shows the expansions obtained with 20 x 20 x 160-mm specimens containing two  
427 aggregate sizes (15% of 315-630 and 15% of 630-1250  $\mu$ m) for the four natures of aggregate.  
428 Only the coefficient of diffusion and the silica content exponent were fitted on these results.  
429 The fitting concerning the final expansion of the siliceous limestone was only performed on  
430 the largest specimens (70x70x280 mm) and for specimens containing only aggregate of the

431 same size. Except for the kinetics of expansion obtained for specimens containing opal, both  
432 kinetics and final expansions obtained by the calculations were in accordance with the  
433 measurements for the four types of aggregate. The description of the expansion kinetics by  
434 the model is globally possible: presence of a latent time before initiation of the expansion,  
435 followed by a high rate of expansion and ending by a low rate to reach the final expansion.

436 Concerning the effect of the alkali concentration of the immersion solution, the difference  
437 between the final expansion predicted by the model (0.70%) and the mean measured  
438 expansion (0.65%) is lower than 10%. The calculation does not show any difference in final  
439 expansions between the three alkali concentrations: the model assumes that all the reactive  
440 silica is consumed in the three conditions and, thus, the volume of ASR gel created is the  
441 same, leading to the same ASR-expansion. The expansion rates obtained by the model at the  
442 beginning of expansion are in good agreement with experiments. This confirms that, in the  
443 case of specimens immersed in alkali solutions, no alkali threshold has to be considered  
444 (unlike for specimens exposed to a saturated environment [34]).

445 The curve obtained by the model for opal did not fit the experimental results well. At the  
446 beginning of the experiment, the slopes of the two curves were the same but, after about 50  
447 days, the measurements showed a speeding-up of the expansions which was not obtained by  
448 the calculation. This can probably be attributed to crack opening for opal specimens as the  
449 specimens containing opal aggregate presented much larger cracks than specimens of the  
450 same size cast with the other aggregates. First, cracks opening increased the apparent  
451 expansion. These cracks could also cause a great increase in diffusion in the specimens, which  
452 could accelerate the reaction.

453 The comparison of the calculated final expansions obtained for the three specimen sizes (20 x  
454 20 x 160 mm, 40 x 40 x 160 mm, 70 x 70 x 280 mm) and the four aggregate sizes of the  
455 siliceous limestone with the measurements is shown in Figures 10 and 11. Concerning these

456 values, only the measurements performed on the largest specimens were used for parameter  
457 identification. The calculated results for all the combinations are in good accordance with the  
458 measurements (Figure 10). The scale effect of ASR expansion pointed out in  
459 experimentations is rather well-predicted (Figure 11). The differences between calculated and  
460 measured expansions are lower than 15% except for the expansions obtained on the smallest  
461 specimens (20x20x160 mm) containing the largest aggregate (1250-2500  $\mu\text{m}$ ), where the  
462 difference is about 30% (Figure 10).

### 463 **3.2.3 Discussion**

464 The molar volume of ASR gel obtained by curve fitting in this work was about 170  $\text{cm}^3/\text{mol}$ .  
465 It was higher than the molar volume obtained in the previous modelling performed for  
466 specimens kept in air at 95% relative humidity [34] and higher than the molar volume of C-S-  
467 H (about 100  $\text{cm}^3/\text{mol}$  [54]). The differences can be explained by the conditions of  
468 conservation (in saturated air in [34] and immersed in NaOH solution in this work) which  
469 could have had a marked effect on the gel morphology and thus on the gels' capability to  
470 absorb water. The ASR gels were produced in pore solution with different water contents and  
471 alkali concentrations. The compositions of the gel were therefore different and thus the molar  
472 volume was different. Concerning the water, ASR gels formed in specimens kept in solution  
473 can absorb much more water than those in humid air (R.H. >95%).

474 The thickness of the connected porous interface zone ( $t_c$  equal to 14.0  $\mu\text{m}$ ) was also higher  
475 than that found in [34], which was about 1  $\mu\text{m}$ . This value was determined to obtain the final  
476 expansions of four aggregate sizes while only two aggregate sizes were studied in the  
477 previous work. The molar volume of the gel was higher and therefore more connected porous  
478 volume was necessary to accommodate the gel. The ASR gels could permeate over a long  
479 distance because the molar volume was high and because the viscosity was small due to high  
480 water and alkali contents. This value is in accordance with the results found in the literature

481 [55-56] showing that the interfacial transition zone between aggregate and cement paste can  
482 reach 20  $\mu\text{m}$ .

## 483 **4. Conclusion**

484 This paper has aimed to investigate and quantify the combined effects of aggregate and  
485 specimen sizes on ASR expansion and the influence of the reactive silica content of aggregate  
486 on this effect. In order to quantify these effects on ASR expansion, a microscopic model was  
487 improved. The main conclusions can be summarized as follows:

488 1. A scale effect, combining the effects of aggregate size, reactive silica content and  
489 specimen size on ASR expansion, has been highlighted by experimentation. A  
490 temporary pessimum size effect had previously been shown to exist due to the speed  
491 of the attack of the reactive silica on the aggregate: the larger the aggregate, the slower  
492 the penetration of ions into the aggregate and thus the slower the expansion [23]. In  
493 this paper, only stabilized expansions were compared, which pointed out another  
494 pessimum effect. The pessimum size effect of stabilized expansion appears not to be  
495 an intrinsic phenomenon of ASR expansion but to depend on the size of the specimen  
496 used to perform the expansion test. For the largest specimens, no pessimum effect was  
497 detected for the aggregate size used in this study. The scale effect has been explained  
498 by fracture mechanics concepts: the larger the ratio between the aggregate and  
499 specimen sizes, the larger the stress intensity factor around the aggregate and the faster  
500 the cracking around the aggregate. After cracking, a part of the ASR gels can be  
501 accommodated by cracks.

502 2. Considering that the scale effect is unavoidable for experimental specimens (the ratio  
503 between specimen and aggregate sizes should be larger than 100 to significantly  
504 decrease the effect), the results of expansion tests should be analysed with respect to

505 this effect. The modelling proposed took the scale effect into account through an  
506 empirical relationship considering underlying linear fracture mechanics concepts.  
507 Calculations are in good accordance with experiments for expansion tests performed  
508 with ratios higher than 10 between specimen and aggregate sizes for the four  
509 aggregates studied.

510 Finally, this paper points out the complexity of ASR expansion and states the numerous  
511 parameters that have to be taken into account to obtain relevant calculations. Another  
512 important conclusion is that stress-free expansions obtained on specimens cannot be directly  
513 used as input parameters in structural models because they are strongly dependent on the  
514 specimen size and on the conservation conditions during the expansion test. To be used,  
515 stress-free expansion test results should be interpreted by considering the phenomena pointed  
516 out in this work. Such an approach is possible: free expansion tests can be carried out to  
517 assess the AAR advancement in aggregates, while the expansion in the conditions of the  
518 damaged structures is assessed through a finite element inverse analysis able to combine the  
519 fitting of the expansion measured on structures with the chemical advancement kinetics  
520 deduced from laboratory tests [57].

## 521 **Acknowledgements**

522 The authors are grateful to Pr Eric Garcia-Diaz, Pr Benoît Fournier, Pr William Prince, Mr  
523 Eric Bourdarot and Mr Etienne Grimal for their advice and suggestions, which have helped to  
524 improve the analysis and the modelling.

## 525 **References**

- 526 [1] S. Dent Glasser, N. Kataoka, The chemistry of alkali-aggregate reaction, Cement and  
527 Concrete Research, 11 (1) (1981) 1-9.  
528 [2] R. Dron, F. Brivot, Thermodynamic and kinetic approach to the alkali-silica reaction.  
529 Part 2: Experiment, Cement and Concrete Research, 23 (1) (1993) 93-103.  
530 [3] T. Ichikawa, M. Miura, Modified model of alkali-silica reaction Cement and Concrete  
531 Research, 37 (9) (2007) 1291-1297.  
532 [4] T. Ichikawa, Alkali-silica reaction, pessimum effects and pozzolanic effect, Cement  
533 and Concrete Research, 39(8) (2009) 716-726.

- 534 [5] D. McConnell, R.C. Mielenz, W. Y. Holland, K.T. Greene, Cement-aggregate reaction  
535 in concrete, Journal of the American Concrete Institute, Proceedings Vol.44, No.2, October  
536 1947, pp.93-128.
- 537 [6] T.M. Kelly, L. Schuman, F.B. Hornibrook, A study of alkali-silica reactivity by means  
538 of mortar bar expansions, Journal of the American Concrete Institute, Proceedings Vol.45,  
539 No.1, September 1948, pp.57-80.
- 540 [7] S. Diamond, N. Thaulow, A study of expansion due to alkali-silica reaction as  
541 conditioned by the grain size of the reactive aggregate, Cement and Concrete Research,4 (4)  
542 (1974) 591-607.
- 543 [8] S. Sprung, Influence of the alkali-aggregate reaction in concrete, Symposium on  
544 Alkali-Aggregate Reaction – Preventive Measures, Icelandic Building Research Institute and  
545 State Cement Works, Reykjavik, Iceland, 1975, pp.231-244.
- 546 [9] D. W. Hobbs, W. Gutteridge, Particle size of aggregate and its influence upon the  
547 expansion caused by the alkali-silica reaction, Magazine of Concrete research, 31 (109)  
548 (1979) 235-242.
- 549 [10] D. Lenzner, U. Ludwig, Alkali aggregate reaction with opaline sandstone, 7<sup>th</sup>  
550 International Congress on the Chemistry of Cement, Septima (Ed.), Paris, France, 1980,  
551 Vol.3, pp.VII-119 - VII-123.
- 552 [11] M. Kawamura, K. Takemoto, S. Hasaba, Application of quantitative EDXA analyses  
553 and microhardness measurements to the study of alkali-silica reaction mechanisms, 6<sup>th</sup>  
554 International Conference of Alkalies in Concrete, Idorn G.M. and Rostam S. (Editors),  
555 Copenhagen, Denmark, 1983, pp.167-174.
- 556 [12] G. Baronio, M. Berra, L. Montanaro, A. Delmastro, A. Bacchiorini, Couplage d'action  
557 de certains paramètres physiques sur le développement de la réaction alcalis-granulats, From  
558 Materials Science to Construction Materials Engineering, 1<sup>st</sup> International RILEM Congress  
559 on Durability of Construction Materials, Versailles, France, 1987, Vol.3, pp 919-926.
- 560 [13] X. Zhang, G. W. Groves, The alkali-silica reaction in OPC-silica glass mortar with  
561 particular reference to pessimum effects, Advances in Cement Research 3 (9) (1990) 9-13.
- 562 [14] C. Zhang, A. Wang, M. Tang, B. Wu, N. Zhang, Influence of aggregate size and  
563 aggregate size grading on ASR expansion, Cement and Concrete Research, 29 (9) (1999)  
564 1393-1396.
- 565 [15] A. Shayan, Value-added Utilisation of Waste Glass in Concrete, IABSE Symposium  
566 Melbourne 2002.
- 567 [16] Z. Xie, W. Xiang, Y. Xi, ASR Potentials of Glass Aggregates in Water-Glass  
568 Activated Fly Ash and Portland Cement Mortars, Journal of Materials in Civil Engineering,15  
569 (1) (2003) 67-74.
- 570 [17] T. Kuroda, S. Nishibayashi, S. Inoue, A. Yoshino, Effects of the particle size of  
571 reactive fine aggregate and accelerated test conditions on ASR expansion of mortar bar,  
572 Transactions of the Japan Concrete Institute, 22 (2000) 113-118.
- 573 [18] Y. Shao, T. Lefort, S. Moras, D. Rodriguez, Studies on concrete containing ground  
574 waste glass, Cement and Concrete Research, 30 (1) (2000) 91-100.
- 575 [19] T. Kuroda, S. Inoue, A. Yoshino, S. Nishibayashi, Effects of particle size, grading and  
576 content of reactive aggregate on ASR expansion of mortars subjected to autoclave method,  
577 12<sup>th</sup> International Conference on Alkali-Aggregate Reaction in Concrete, Tang M. and Deng  
578 M. (Editors), Beijing, China, 2004, pp.736-743.
- 579 [20] K. Ramyar, A. Topal, O. Andic, Effects of aggregate size and angularity on alkali-  
580 silica reaction, Cement and Concrete Research, 35 (2005) 2165-2169.
- 581 [21] M. Moisson, M. Cyr, E. Ringot, A. Carles-Gibergues, Efficiency of reactive aggregate  
582 powder in controlling the expansion of concrete affected by alkali-silica reaction (ASR), 12th



583 International Conference on Alkali-Aggregate Reaction in Concrete, Tang M. and Deng M.  
584 (Editors), Beijing, China, 2004, pp.617-624.

585 [22] S. Multon, M. Cyr, A. Sellier, N. Leklou, L. Petit, Coupled effects of aggregate size  
586 and alkali content on ASR expansion, *Cement and Concrete Research*, 38 (2008) 350-359.

587 [23] S. Multon, M. Cyr, A. Sellier, P. Diederich, L. Petit, Effect of aggregate size and  
588 alkali content on ASR expansion, *Cement and Concrete Research*, 40 (2010) 508–516.

589 [24] C.F. Dunant, K.L. Scrivener, Effects of aggregate size on alkali–silica-reaction  
590 induced expansion, *Cement and Concrete Research* 42 (6) (2012) 745–751.

591 [25] RFM Bakker, The influence of test specimen dimensions on the expansion of reactive  
592 alkali aggregate in concrete. Proceedings of the 6th ICAAR, Copenhagen, Denmark, 1983,  
593 pp. 369-375.

594 [26] C. Zhang, A. Wang, M. Tang, N. Zhang, Influence of dimension of test specimen on  
595 alkali aggregate reactive expansion, *ACI Materials Journal*, 96 (1999) 204-207.

596 [27] J. Duchesne, M-A. Bérubé, Effect of the cement chemistry and the sample size on  
597 ASR expansion of concrete exposed to salt, *Cement and Concrete Research*, 33 (2003) 629–  
598 634.

599 [28] N. Smaoui, M-A. Bérubé, B. Fournier, B. Bissonnette, Influence of specimen  
600 geometry, direction of casting, and mode of concrete consolidation on expansion due to ASR.  
601 *Cement, Concrete and Aggregate*, 26 (2004) 58-70.

602 [29] P. Goltermann, Mechanical predictions on concrete deterioration. part 1: Eigenstresses  
603 in concrete, *ACI Materials Journal*, 91 (6) (1994) 543–550.

604 [30] Z.P Bazant, A. Steffens, Mathematical model for kinetics of alkali-silica reaction in  
605 concrete, *Cement and Concrete Research*, 30 (2000) 419–428.

606 [31] I. Comby-Perot, F. Bernard, P.-O. Bouchard, F. Bay, E. Garcia-Diaz, Development  
607 and validation of a 3D computational tool to describe concrete behaviour at mesoscale.  
608 Application to the alkali-silica reaction, *Computational Material Science*, 46 (4) (2009) 1163-  
609 1177.

610 [32] C.F. Dunant, K.L. Scrivener, Micro-mechanical modelling of alkali–silica-reaction  
611 induced degradation using the AMIE framework, *Cement and Concrete Research* 40 (4)  
612 (2010) 517–525.

613 [33] Y. Furusawa, H. Ohga, T. Uomoto, An analytical study concerning prediction of  
614 concrete expansion due to alkali-silica reaction, in Malhotra (ed.), 3<sup>rd</sup> International  
615 Conference on Durability of Concrete, Nice, France, 1994, pp 757–780.

616 [34] S. Multon, A. Sellier, M. Cyr, Chemo–mechanical modeling for prediction of alkali  
617 silica reaction (ASR) expansion, *Cement and Concrete Research*, 39 (2009) 490-500.

618 [35] S. Poyet, A. Sellier, B. Capra, G. Foray, J.-M. Torrenti, H. Cognon, E. Bourdarot,  
619 Chemical modelling of Alkali Silica reaction: Influence of the reactive aggregate size  
620 distribution, *Materials and Structures*, 40 (2007) 229–239.

621 [36] A. Nielsen, F. Gottfredsen, F. Thogersen, Development of stresses in concrete structures  
622 with alkali-silica reactions, *Material and Structures*, 26 (1993) 152-158.

623 [37] A. Sellier, J-P. Bournazel, A. Mébarki, Modelling the alkali aggregate reaction within a  
624 probabilistic frame-work, 10<sup>th</sup> International Conference of Alkali Aggregate Reaction,  
625 Melbourne, Australia, 1996, pp 694-701.

626 [38] A. Suwito, W. Jin, Y. Xi, C. Meyer, A mathematical model for the pessimum effect of  
627 ASR in concrete, *Concrete Science and Engineering*, 4 (2002) 23-34.

628 [39] A. Sellier, J-P. Bournazel, A. Mébarki, Une modélisation de l'alkali-réaction intégrant  
629 une description des phénomènes aléatoires locaux, *Materials and Structures* 28 (1995) 373-  
630 383.

631 [40] L. Charpin, A. Ehrlacher, A computational linear elastic fracture mechanics-based  
632 model for alkali–silica reaction, *Cement and Concrete Research*, 42 (4) (2012) 613-625.

633 [41] H.W. Reinhardt, O. Mielich, A fracture mechanics approach to the crack formation in  
634 alkali-sensitive grains, *Cement and Concrete Research*, 41 (3) (2011) 255-262.

635 [42] X.X. Gao, S. Multon, M. Cyr, A. Sellier, Optimising an expansion test for the  
636 assessment of alkali-silica reaction in concrete structures, *Materials and Structures*, 44 (2011)  
637 1641–1653.

638 [43] X.X. Gao, Contribution to the requalification of Alkali Silica Reaction (ASR)  
639 damaged structures: Assessment of the ASR advancement in aggregates, PhD thesis, 2010,  
640 Université de Toulouse, France.

641 [44] J. Lemaître, J-L. Chaboche, *Mécanique des Matériaux Solides*, Dunod (Eds.), Paris,  
642 France, 1988.

643 [45] D. François, A. Pineau, A. Zaoui, *Comportement mécanique des matériaux :  
644 viscoplasticité, endommagement, mécanique de la rupture, mécanique du contact*, Hermes  
645 Eds, 1993.

646 [46] V. Saouma, L. Perotti, Constitutive model for alkali-aggregate reactions, *ACI  
647 Materials Journal*, 103 (3) (2006) 194-202.

648 [47] E. Garcia-Diaz, J. Riche, D. Bulteel, C. Vernet, Mechanism of damage for the alkali-  
649 silica reaction, *Cement and Concrete Research*, 36 (2006) 395 – 400.

650 [48] M. Ben Haha, E. Gallucci, A. Guidoum, K.L. Scrivener, Relation of expansion due to  
651 alkali silica reaction to the degree of reaction measured by SEM image analysis, *Cement and  
652 Concrete Research* 37 (2007) 1206–1214.

653 [49] D.W. Hobbs, Deleterious alkali-silica reactivity in the laboratory and under field  
654 conditions, *Magazine of Concrete Research* 45 (163) (1993) 103–112.

655 [50] C. A. Rogers, R. D. Hooton, Reduction in Mortar and Concrete Expansion with  
656 Reactive Aggregates Due To Alkali Leaching, *Cement, Concrete and Aggregates* 13(1) (1991)  
657 42-49.

658 [51] M.H. Shehata, M.D.A. Thomas, The effect of fly ash composition on the expansion of  
659 concrete due to alkali-silica reaction, *Cement and Concrete Research* 30 (7) (2000) 1063–  
660 1072.

661 [52] M.D.A. Thomas, B.Q. Blackwell, P.J. Nixon, Estimating the alkali contribution from fly  
662 ash to expansion due to alkali-aggregate reaction in concrete, *Magazine of Concrete Research*  
663 48 (177) (1996) 251–264.

664 [53] S. Goto, D. M. Roy, Diffusion of ions through hardened cement pastes *Cement and  
665 Concrete Research*, 11 (5–6) (1981) 751-757.

666 [54] H.F.W. Taylor, *Cement Chemistry*, Academic Press, London, 1990.

667 [55] K. L. Scrivener, K. M. Nemati, The percolation of pore space in the cement  
668 paste/aggregate interfacial zone of concrete, *Cement and Concrete Research* 26(1) (1996) 35-  
669 40.

670 [56] K. L. Scrivener, A. K. Crumbie, P. Laugesen, The interfacial transition zone (ITZ)  
671 between cement paste and aggregate in concrete, *Interface science* 12 (2004) 411-421.

672 [57] A. Sellier, E. Bourdarot E., S. Multon, M. Cyr, E. Grimal, Combination of structural  
673 monitoring and laboratory tests for the assessment of AAR-swelling: application to a gate  
674 structure dam, *ACI Materials Journal* 106 (3) (2009) 281-290.

675

676

677

678 **TABLES**

679

680

681

*Table 1: Reactive silica contents of different aggregates [43]*

<i>Reactive silica (SiO<sub>2</sub>)</i>	<i>SL</i>	<i>O</i>	<i>Q</i>	<i>QA</i>
<i>Percentage by mass (%)</i>	6.9	50.4	7.6	2.7
<i>Content (mol/m<sup>3</sup> of aggregate)</i>	3000	21900	3300	1170

682

683

*Table 2: Parameters of model*

<b>Parameter</b>	<b>Symbol</b>	<b>Identification</b>	<b>Value</b>	<b>Units</b>
<i>Aggregate</i>				
Reactive silica content	<i>s</i>	measurement	D.N.A.*	mol/m <sup>3</sup>
Coefficient of diffusion	<i>D<sub>a</sub></i>	curve fitting	D.N.A.*	m <sup>2</sup> /s
Porosity	<i>p</i>	usual value	0.01	%
<i>Paste</i>				
Porosity of mortar	<i>p<sub>mort</sub></i>	measurement	18.0	%
Thickness of the connected porous interface zone	<i>t<sub>c</sub></i>	curve fitting	14.0 x 10 <sup>-6</sup>	m
<i>Gel</i>				
Molar volume of ASR gel	<i>V<sub>gel</sub><sup>mol</sup></i>	curve fitting	1.7 x 10 <sup>-4</sup>	m <sup>3</sup> /mol
Scale effect coefficient	<i>c</i>	curve fitting	0.037	(mol/m <sup>3</sup> ) <sup>-χ</sup>
Silica content exponent	<i>χ</i>	curve fitting	0.75	-

684 \* depends on the nature of the aggregate

685

686

687 **FIGURES**

688

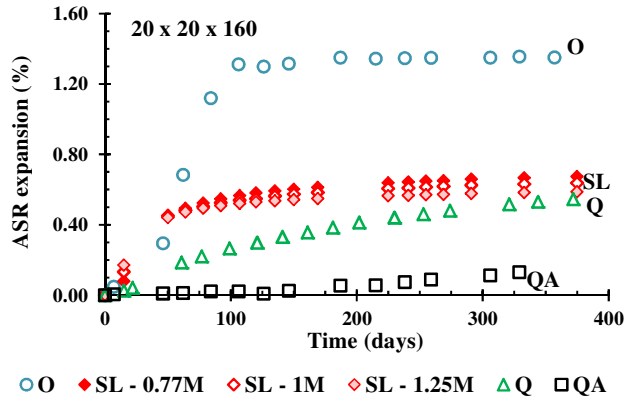


**Figure 1:** ASR expansions according to the alkali concentration of the immersion solution for SL (0.77, 1.0 and 1.25 mol/l) and to the nature of the aggregate (O: opal, SL: siliceous limestone, Q: quartzite and QA: quartz aggregate) stored in the 1 mol/l NaOH immersion solution

689

690



(a)



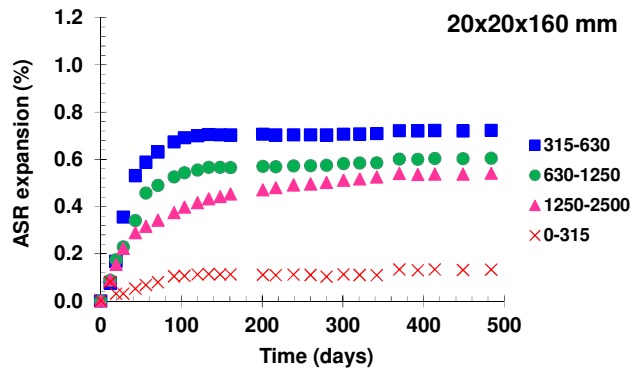
(b)

**Figure 2:** Cracking patterns of specimens cast with the siliceous limestone (a) and with opal (b)

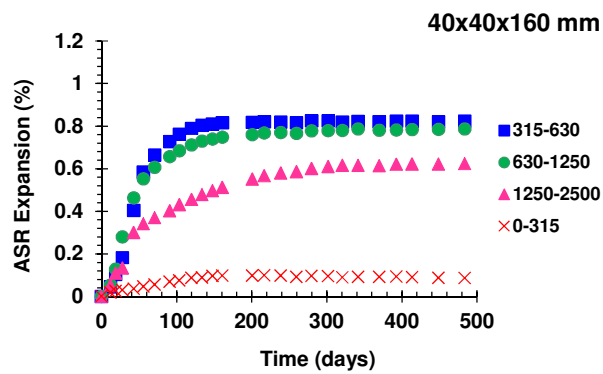
691

692

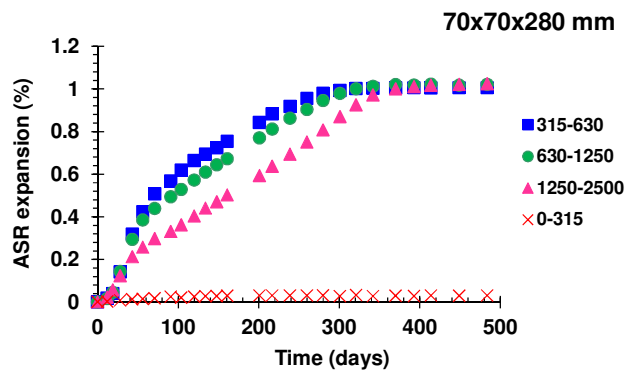
693



(a)



(b)



(c)

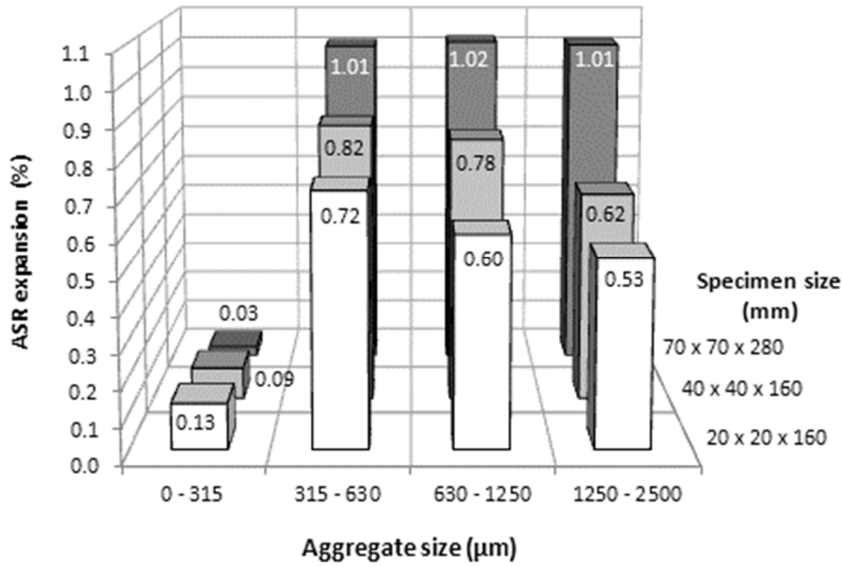
**Figure 3:** ASR expansions on prismatic specimens 20x20x160 mm (a), 40x40x160 mm (b) and 70x70x280 mm (c)

694

695

696

697



698

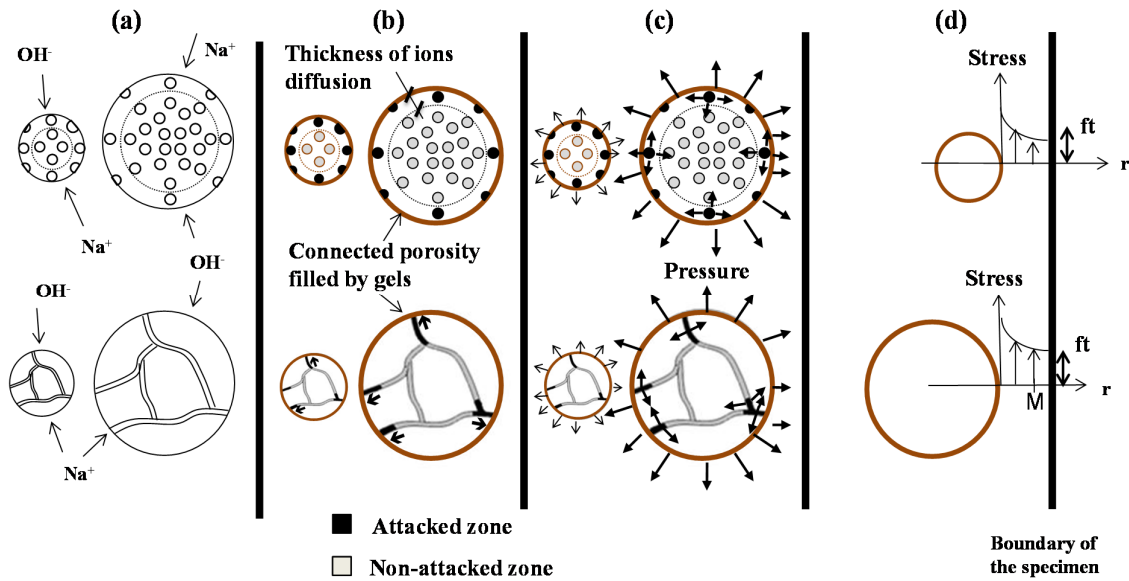
**Figure 4:** Final ASR expansions according to specimens size and aggregates size

699

700

701

702



703

704

705

706

**Figure 5:** Four phases of ASR development: ion diffusion (a), reaction with the reactive silica (b), gel pressure (c), and stress development (d). Top line: diffuse reactive silica distribution, bottom line: veins

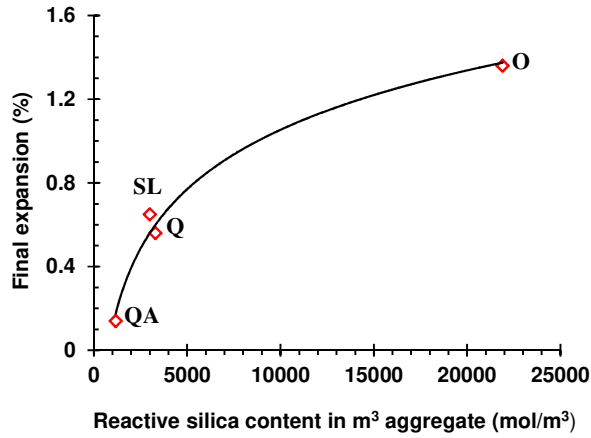


**Figure 6:** Final expansions according to reactive silica content

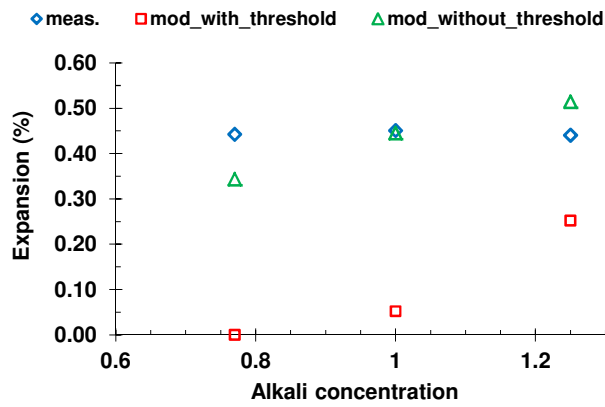


**Figure 7:** Measured and calculated expansions at 50 days according to the alkali concentration of the solution (calculations performed with or without the threshold of 0.625 mol/l)

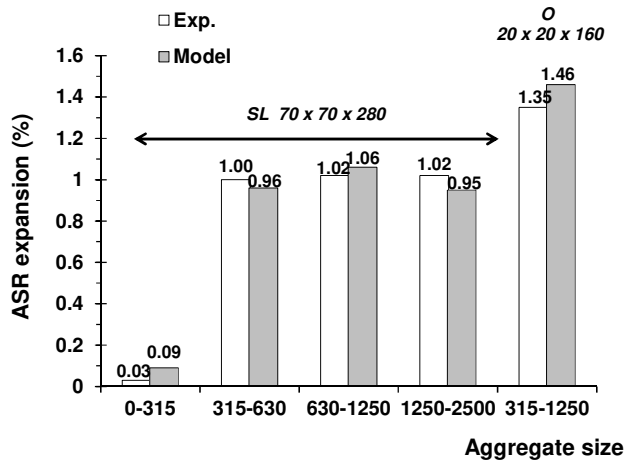


Figure 8: Identification of the modelling parameters

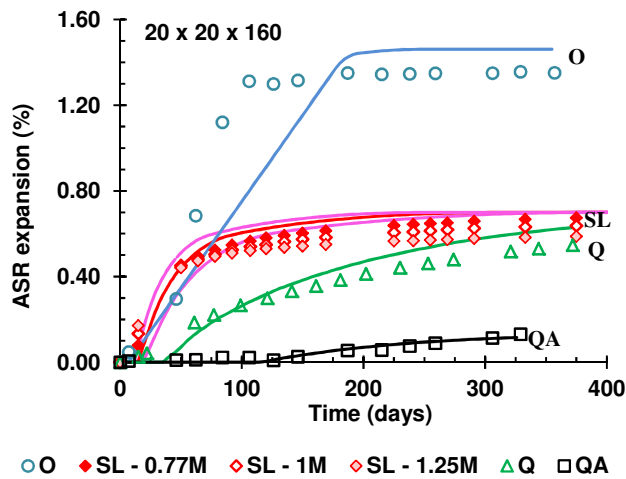
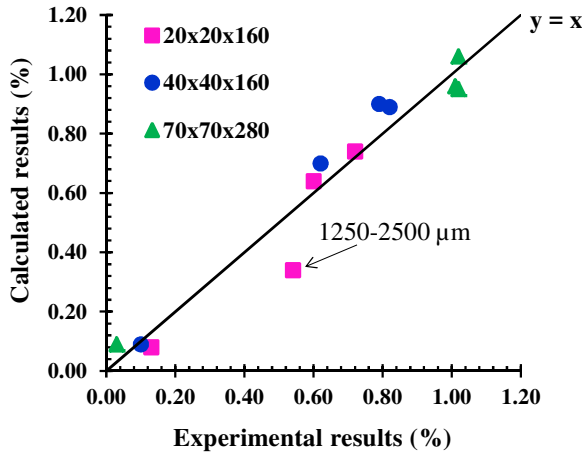


Figure 9: Comparison of calculated and measured expansions according to the alkali concentration of the immersion solution (0.77, 1.0 and 1.25 mol/l) and to the nature of the aggregate (O: opal, SL: siliceous limestone, Q: quartzite and QA: quartz aggregate)

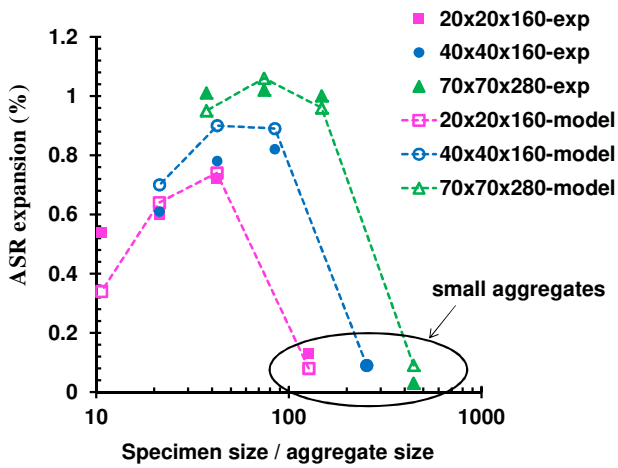
707  
708





709  
710  
711  
712  
713  
714  
715

**Figure 10:** Comparison of calculated and measured final expansions for all the combinations between the sizes of aggregates and specimens with siliceous limestone



716  
717  
718  
719

**Figure 11:** Scale effect of ASR expansion: experimental and modelling results